On the Formation of Gas Giant Planets on Wide Orbits

Alan P. Boss

Department of Terrestrial Magnetism, Carnegie Institution of Washington, 5241 Broad Branch Road, NW, Washington, DC 20015-1305

boss@dtm.ciw.edu

ABSTRACT

A new suite of three dimensional radiative, gravitational hydrodynamical models is used to show that gas giant planets are unlikely to form by the disk instability mechanism at distances of $\sim$ 100 AU to $\sim$ 200 AU from young stars. A similar result seems to hold for the core accretion mechanism. These results appear to be consistent with the paucity of detections of gas giant planets on wide orbits by infrared imaging surveys, and also imply that if the object orbiting GQ Lupus is a gas giant planet, it most likely did not form at a separation of $\sim$ 100 AU. Instead, a wide planet around GQ Lup must have undergone a close encounter with a third body that tossed the planet outward to its present distance from its protostar. If it exists, the third body may be detectable by NASA's *Space Interferometry Mission*.

Subject headings: stars: planetary systems – stars: low-mass, brown dwarfs

1. Introduction

Because radial velocity planet-finding surveys are most sensitive to planets with relatively short-period orbits, the search for gas giant planets on wide orbits (i.e., separations much greater than $\sim$ 10 AU) has been undertaken primarily by direct imaging surveys at infrared wavelengths. These surveys have largely turned up empty-handed: McCarthy & Zuckerman (2004) found no evidence for any planets with masses of 5 to 10 M_J (Jupiter mass) at distances of 75 to 300 AU from $\sim$ 100 stars. Similarly, Masciadri et al. (2005) found nothing in their search of 28 stars for similar-mass planets with separations of at least $\sim$ 36 to $\sim$ 65 AU, as did Lowrance et al. (2005) in their search of 45 nearby stars.

However, recently two ground-based surveys have detected very low mass companions with wide separations. Using the NACO adaptive optics systems on the Very Large Telescope, Chauvin et al. (2004) found a $\sim 5 M_J$ companion to the $\sim 25 M_J$ brown dwarf 2M1207,

with a separation of ~ 60 AU. Neuhauser et al. (2005) used the same NACO system to detect an object orbiting ~ 100 AU from the ~ 1 Myr-old classical T Tauri star GQ Lup. The mass of this object appears to lie between $\sim 1 M_J$ and $\sim 42 M_J$, with a good chance that its mass is low enough ($< 13 M_J$) for it to be classified as a planet rather than as a brown dwarf.

Core accretion (Mizuno 1980), the generally accepted mechanism of gas giant planet formation, encounters difficulties in forming gas giants at distances much greater than ~ 5 AU (Pollack et al. 1996; Inaba, Wetherill, & Ikoma 2003) because of the decreasing surface density of solids available to make the solid cores and the consequent increase in the formation time scale. Forming gas giant planets at distances of ~ 100 AU by core accretion appears to be extremely unlikely.

Observations of the circumstellar disk orbiting the Herbig Ae star AB Aurigae show clear evidence for spiral structures at both near-infrared (Fukagawa et al. 2004) and millimeter-wavelengths (Corder, Eisner, & Sargent 2005). Four trailing spiral arms can be resolved, at distances of 200 AU to 450 AU from the central ~ 4 Myr-old star with a mass of 2.8 $M_\odot$. These observations are perhaps the first direct evidence for large scale gravitational instability in a circumstellar disk, and suggest that the competing mechanism for gas giant planet formation, disk gravitational instability (Cameron 1978; Boss 1997, 2003), might be able to operate at distances of ~ 100 AU or more. This paper examines the latter possibility, by extending the same disk instability models that suggest gas giant planet formation is possible at distances of ~ 10 AU, to examine the case of much larger disks, ~ 100 AU in size.

2. Numerical Methods

The calculations were performed with a finite volume code that solves the three dimensional equations of hydrodynamics and radiative transfer, as well as the Poisson equation for the gravitational potential. The code is second-order-accurate in both space and time (Boss & Myhill 1992) and has been used extensively in previous disk instability studies (e.g., Boss 2003).

The equations are solved on spherical coordinate grids with $N_r = 101$, $N_\theta = 23$ in $\pi/2 \geq \theta \geq 0$, and $N_\phi = 256$ or 512. The radial grid extends from 100 AU to 200 AU with a uniform spacing of $\Delta r = 1$ AU. The θ grid is compressed toward the midplane in order to ensure adequate vertical resolution ($\Delta\theta = 0.3^o$ at the midplane). The ϕ grid is uniformly spaced to prevent any azimuthal bias. The central protostar wobbles in response to the

growth of disk nonaxisymmetry, preserving the location of the center of mass of the star and disk system. The number of terms in the spherical harmonic expansion for the gravitational potential of the disk is $N_{Ylm} = 32$ or 48. The Jeans length criterion is monitored throughout the calculations to ensure proper spatial resolution: the numerical grid spacings in all three coordinate directions always remain less than 1/4 of the local Jeans length.

The boundary conditions are chosen at both 100 AU and 200 AU to absorb radial velocity perturbations. Mass and linear or angular momentum entering the innermost shell of cells at 100 AU is added to the central protostar and thereby removed from the hydrodynamical grid. Similarly, mass and momentum that reaches the outermost shell of cells at 200 AU is effectively removed from the calculation: the mass piles up in this shell and is assigned zero radial velocity. The inner and outer boundary conditions are designed to absorb incident mass and momentum, rather than to reflect mass and momentum back into the main grid. The angular momentum added to the central protostar is used only to monitor the conservation of total angular momentum during the calculation.

As in Boss (2003), two of the models treat radiative transfer in the diffusion approximation, with no radiative losses or gains occuring in regions where the vertical optical depth τ drops below 10. In very low density regions, the disk temperature is assumed to be the same as that of the disk envelope, 30K. The energy equation is solved explicitly in conservation law form, as are the four other hydrodynamic equations.

3. Initial Conditions

The models calculate the evolution of a $1 M_{\odot}$ central protostar surrounded by a protoplanetary disk with a mass of 0.16 $M_{\odot}$ between 100 AU and 200 AU. The models envision planet formation as occurring during the embedded phase of star formation, when the star is a Class I object still accreting mass from the infalling cloud envelope onto a relatively massive protoplanetary disk. Given that the disk mass interior to 100 AU would add another $\sim 0.1 M_{\odot}$, the total amount of circumstellar matter is assumed to be perhaps unrealistically high, making the negative results regarding forming gas giants by disk instability at such large distances obtained here even stronger than would be the case for an assumed lower mass disk system.

The initial protoplanetary disk structure is based on the following approximate vertical density distribution (Boss 1993) for an adiabatic, self-gravitating disk of arbitrary thickness in near-Keplerian rotation about a point mass M_s

$$\rho(R,Z)^{\gamma-1} = \rho_o(R)^{\gamma-1}$$
$$-\Big(\frac{\gamma-1}{\gamma}\Big)\Big[\Big(\frac{2\pi G\sigma(R)}{K}\Big)Z + \frac{GM_s}{K}\Big(\frac{1}{R} - \frac{1}{(R^2+Z^2)^{1/2}}\Big)\Big],$$

where R and Z are cylindrical coordinates, $\rho_o(R)$ is a specified midplane density, and $\sigma(R)$ is a specified surface density. The disk's surface is defined by locations where the density distribution defined above falls to zero; regions where the density falls below zero are outside the disk. The adiabatic pressure (used only for defining the initial model – the radiative transfer solution includes a full thermodynamical treatment) is defined by $p = K\rho^\gamma$, where K is the adiabatic constant and γ is the adiabatic exponent. The adiabatic constant is $K = 5.1 \times 10^{17}$ (cgs units) and $\gamma = 5/3$ for the initial model. K was chosen to be three times larger than in the previous disk instability models in order to produce a thicker outer disk. The radial variation of the midplane density is a power law that ensures near-Keplerian rotation throughout the disk

$$\rho_o(R) = \rho_{o4}\Big(\frac{R_4}{R}\Big)^{3/2},$$

where $\rho_{o4} = 4.0 \times 10^{-11}$ g cm^{-3} and $R_4 = 4$ AU. With this assumption for $\rho_o(R)$, the initial disk surface density profile from 100 AU to 200 AU is $\sigma_i \propto r^{-2}$, a steeper falloff than occurs for this choice of an initial disk model at radii of ~ 20 AU, where $\sigma_i \propto r^{-3/2}$ (Boss 2002). A low density halo ρ_h of gas and dust infalls onto the disk, with

$$\rho_h(r) = \rho_{h4} cos^2(\theta)\Big(\frac{R_{100}}{r}\Big)^{3/2},$$

where $\rho_{h4} = 4.5 \times 10^{-15}$ g cm^{-3}, $R_{100} = 100$ AU, and r is the spherical coordinate radius. The initial envelope mass is 0.05 $M_\odot$.

Three initially uniform disk temperatures are investigated, $T_o = 20$, 25, and 30K. With the assumed initial density profile, the disks have initial Q gravitational stability parameters as low as $Q_{min} = 1.3$ for $T_o = 20$K and $Q_{min} = 1.6$ for $T_o = 30$K. In low optical depth regions such as the disk envelope, the temperature is assumed to be 30 K. The Rosseland mean opacities used in the radiative transfer solution have been updated to include the dust grain opacities calculated by Pollack et al. (1994).

4. Results

Table 1 lists the initial conditions for the models as well as the final times (t_f) to which they were evolved. Note that for the initial disk, the orbital period is 740 yrs at 100 AU and 2400 yrs at 200 AU, so the $N_\phi = 256$ models were evolved for times that varied between ~ 10 and ~ 110 orbital periods at 100 AU, while the $N_\phi = 512$ models were calculated for between ~ 5 and ~ 27 orbital periods at 100 AU.

Models A and AH began with a minimum Q parameter of 1.30, and thus had a greater tendency toward instability than models C and CH, where the initial minimum Q value was 1.59, implying initial marginal gravitational instability. Models B and BH were intermediate with a value of 1.45. Models A and AH were evolved with the usual radiative transfer procedures, but it was found to be necessary for numerical stability to evolve the other four models (B, BH, C, CH) with the disk temperature fixed at its initial value. The latter assumption errs on the side of encouraging clump formation, compared to the full thermodynamical treatment in models A and AH, but we shall see that even this assumption does not result in clump formation.

Figure 1 shows the result of model AH after 4000 yrs of evolution. A tightly wound set of spiral arms has formed, but no dense clumps capable of contracting to become self-gravitating protoplanets appear, nor do any appear during the earlier phases of the evolution. This is in spite of the fact that model AH is the model that should be most likely to form clumps if clump formation is possible, given its low initial minimum value of $Q = 1.30$ and its relatively high spatial resolution ($N_\phi = 512$).

The main reason why clumps do not form in this model (as well as the others) appears to be that rapid inward transport of mass associated with the gravitational torques between the growing spiral arms is able to deplete the inner disk gas before it can become dense enough to form gravitationally-bound clumps. This is evident in Figure 2, which shows how the disk in model AH has developed a severe inner depletion of gas that renders the disk locally gravitationally stable by a large factor. The relatively steep decrease in disk surface density at these distances ($\sigma_i \propto r^{-2}$) means that the loss of the innermost disk gas drives the disk toward stability.

The tightness of the spiral arms in model AH is further illustrated in Figure 3, which shows the equatorial temperature contours at the same time as Figure 1. The spiral arms are delineated by sharply defined, tightly wound temperature maxima that occur where the disk gas is being compressed locally. The fact that the spiral structures that form are so tightly wound appears to also work against clump formation, as this configuration prevents the superposition of multiple spiral arms that would lead to locally higher gas densities, a

process that occurs frequently in disk instability models on scales of $\sim$ 10 AU (e.g., Boss 2003) and helps lead to gravitationally-bound clump formation. The spiral arms in Boss (2003) are loosely wound in comparison to those seen in Figures 1 and 3. In the latter models, clumps formed within $\sim$ 300 yrs, or $\sim$ 3 orbital periods at $\sim$ 20 AU.

Given the failure of model AH to produce any dense clumps, it should be obvious that in the remaining five models, clump formation is even more inhibited by the same processes that afflicted model AH. This is in spite of the fact that in models B, BH, C, and CH, the disk was assumed to remain isothermal during the evolution for numerical reasons, an assumption that can be expected to err on the side of clump formation. Figure 4 shows that in model CH, with an initial minimum value of $Q = 1.59$ and $N_\phi = 512$, the disk becomes remarkably axisymmetric after its inner regions have been depleted by accretion onto the central protostar.

5. Conclusions

These models have shown that the disk instability mechanism has great difficulty forming gas giant planets *in situ* at distances of $\sim$ 100 AU to $\sim$ 200 AU from solar-mass protostars. The models presented here show no clump formation, even in an initially marginally gravitationally unstable disk. Given that the core accretion mechanism is even more hampered in forming gas giant planets at $\sim$ 100 AU distances (Pollack et al. 1996; Inaba, Wetherill & Ikomoa 2003), it seems clear that gas giant planets do not appear to be able to form on such wide orbits, consistent with the failure of most direct imaging surveys to detect massive gas giant planets (McCarthy & Zuckerman 2004; Masciadri et al. 2005; Lowrance et al. 2005).

On the other hand, the detection of the wide, very low mass objects around 2M1207 by Chauvin et al. (2004) and around GQ Lup by Neuhauser et al. (2005) demands an explanation. The 2M1207 system would seem to be best explained as a binary system composed of a brown dwarf and a sub-brown dwarf, with a mass ratio $q = 0.2$, similar to that of many binary star systems. Binary and multiple star systems are generally believed to have formed from the collapse and fragmentation of dense molecular clouds, a process that precedes the planet formation processes considered here.

If the very low mass companion to GQ Lup turns out to have a mass close to the upper limit of $\sim 42 M_J$, then it also most likely formed as a brown dwarf companion to GQ Lup through collapse and fragmentation into a binary system with $q \leq 0.06$ (assuming a mass of $\sim 0.7 M_\odot$ for the T Tauri star GQ Lup). However, if the object has a much lower mass, implying that it did not form by fragmentation, but through the planet formation process

in a protoplanetary disk, it is hard to see how such an object could have formed *in situ* at $\sim$ 100 AU by either core accretion or disk instability. Instead, one would be forced to consider a scenario where the object formed much closer to GQ Lup, perhaps within $\sim$ 30 AU (e.g., Boss 2003), and then was flung outward on a highly eccentric orbit to $\sim$ 100 AU by a close encounter with another body in the GQ Lup system (cf., Debes & Sigurdsson 2006). Outward scattering of planets to wide orbits is a likely possibility in crowded systems of giant planets (Adams & Laughlin 2003).

NASA's *Space Interferometry Mission (SIM)* should be able to detect such a third body orbiting relatively close to GQ Lup, if it exists, settling the question of the origin of the putative planet's wide orbit. GQ Lup has a V magnitude of 14.4 but is highly reddened, allowing *SIM* to perform narrow angle astrometry on it in the R band. Because the third body would be left on a tighter orbit around GQ Lup as a result of the close encounter with the planet now on a wide orbit, the third body would be expected to be on a relatively short period orbit that could be detected during *SIM's* nominal mission lifetime of 5 yrs. At GQ Lup's distance of 140 pc, *SIM* would be able to detect a third body with a mass as low as $\sim 1 M_J$ orbiting with a semi-major axis of 10 AU or less. As the third body is likely to be significantly more massive than the wide planet, *SIM* should be able to detect this hypothetical object.

I thank Alycia Weinberger for motivating these calculations, Charles Beichman for advice about *SIM's* capabilities, Fred Adams for his excellent comments on the manuscript, and Sandy Keiser for her extraordinary computer systems expertise. This research was supported in part by NASA Planetary Geology and Geophysics grant NNG05GH30G and by NASA Astrobiology Institute grant NCC2-1056. The calculations were performed on the Carnegie Alpha Cluster, the purchase of which was partially supported by NSF Major Research Instrumentation grant MRI-9976645.

REFERENCES

Adams, F. C, & Laughlin, G. 2003, Icarus, 163, 290

Boss, A. P. 1993, ApJ, 417, 351

——. 1997, Science, 276, 1836

——. 2002, ApJ, 576, 462

——. 2003, ApJ, 599, 577

Boss, A. P., & Myhill, E. A. 1992, ApJS, 83, 311

Cameron, A. G. W. 1978, Moon Planets, 18, 5

Chauvin, G., et al. 2004, A&A, 425, L29.

Corder, S., Eisner, J., & Sargent, A. 2005, ApJ, 622, L133

Debes, J. H., & Sigurdsson, S. 2006, A&A, submitted

Fukagawa, M., et al. 2004, ApJ, 605, L53

Inaba, S. , Wetherill, G. W., & Ikoma, M. 2003, Icarus, 166, 46

Lowrance, P. J., et al. 2005, AJ, 130, 1845

Masciadri, E., et al. 2005, ApJ, 625, 1004

McCarthy, C., & Zuckerman, B. 2004, AJ, 127, 2871

Mizuno, H. 1980, Prog. Theor. Phys., 64, 544

Neuhauser, R., et al. 2005, A&A, 435, L13.

Pollack, J. B., et al. 1994, ApJ, 421, 615

——. 1996, Icarus, 124, 62

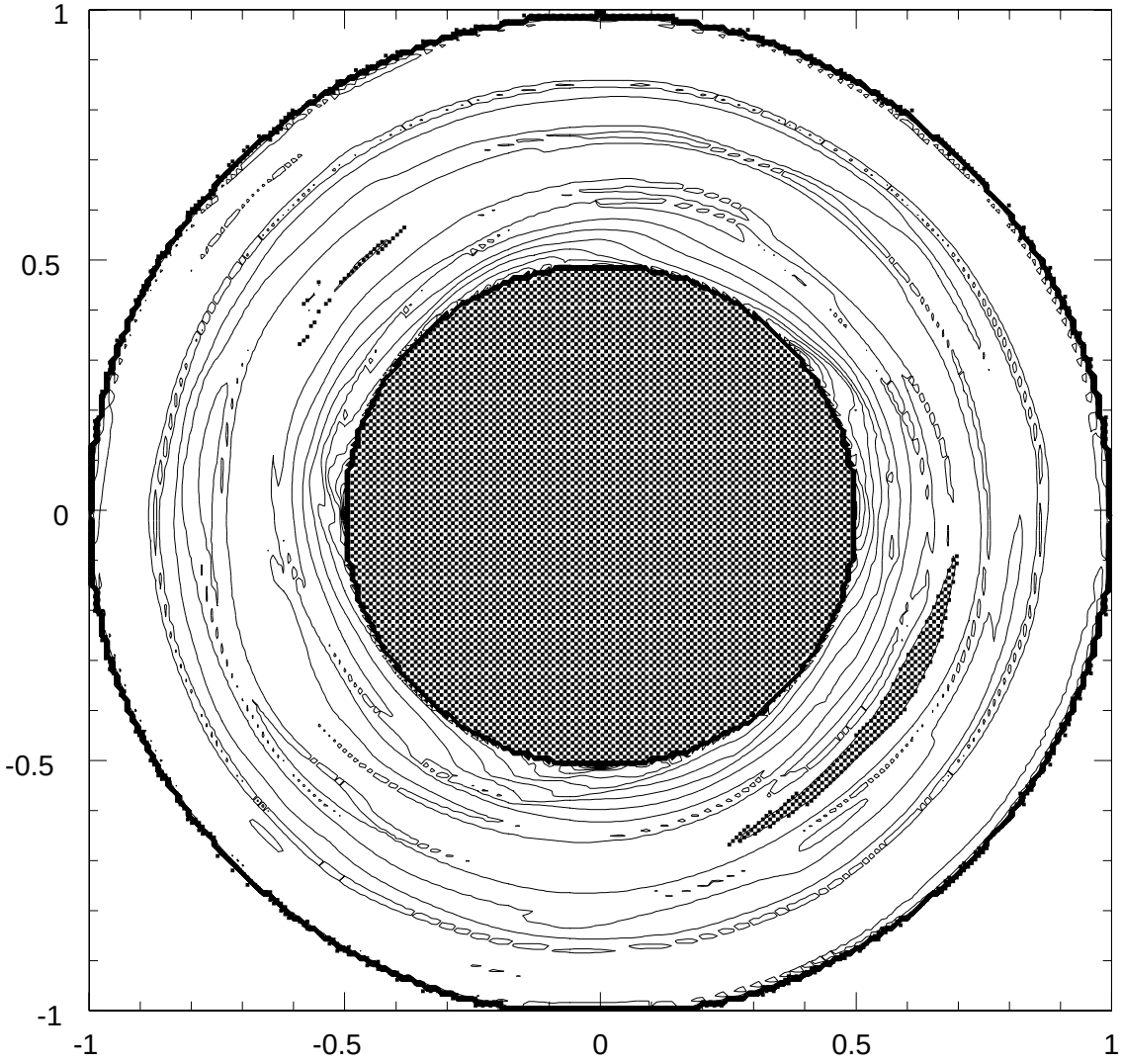

Fig. 1.— Equatorial density contours for model AH after 4000 yrs of evolution. In this figure as well as in the subsequent figures, a $0.16 M_\odot$ disk is in orbit around a central 1 $M_\odot$ protostar. The entire disk is shown, with an outer radius of 200 AU and an inner radius of 100 AU, through which mass accretes onto the central protostar. Hashed regions denote spiral arms with densities higher than 3.2×10^{-14} g cm^{-3}. Density contours represent factors of two change in density.

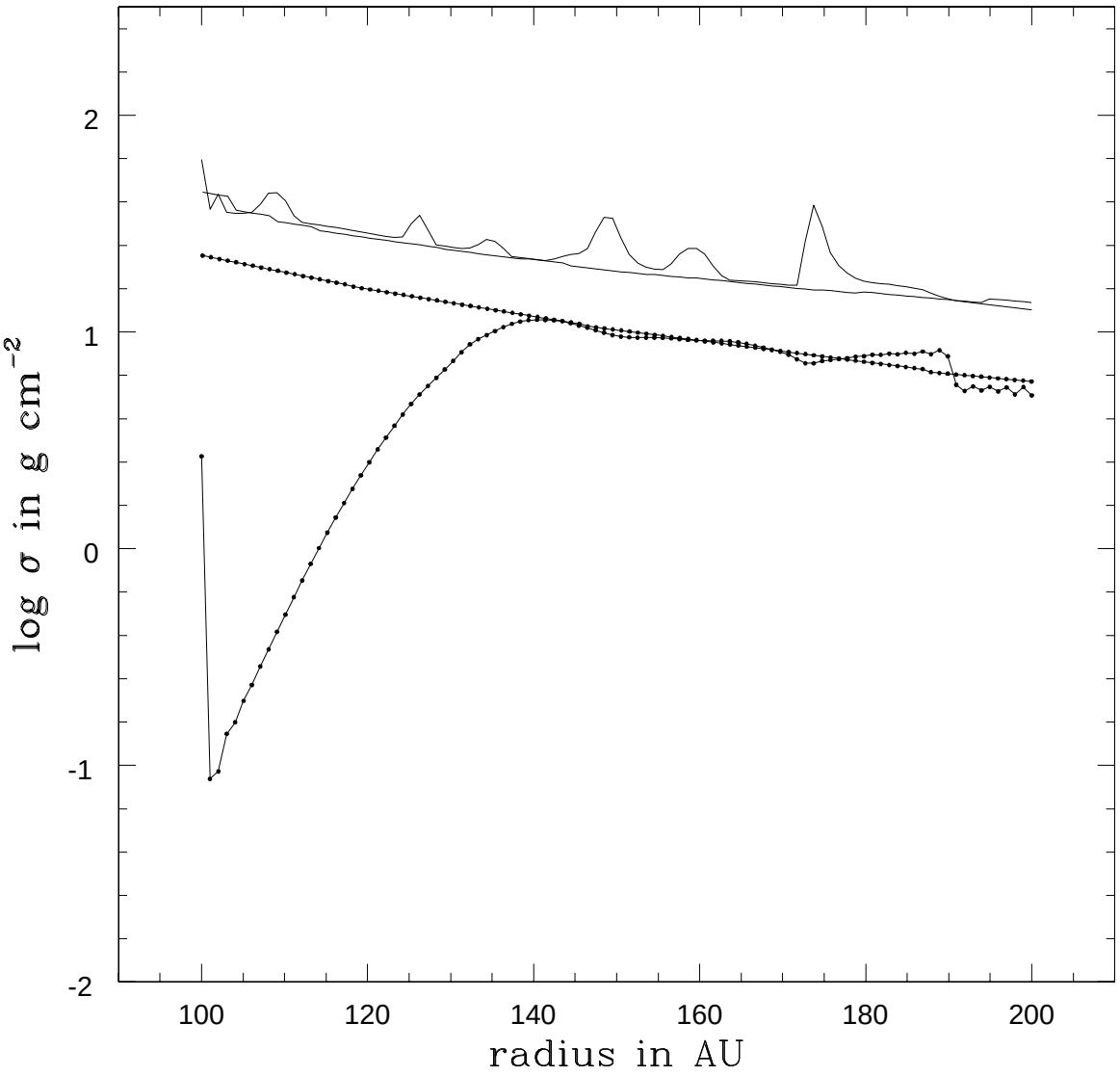

Fig. 2.— Radial (azimuthally averaged) profiles for the disk gas surface density (dots) in the initial model AH and after 4000 yrs of evolution, compared to the surface densities needed for $Q = 1$ (solid line) at both times. The smoother curves are the initial profiles for both quantities. After 4000 yrs, the innermost disk gas has been largely accreted inside the inner 100 AU boundary.

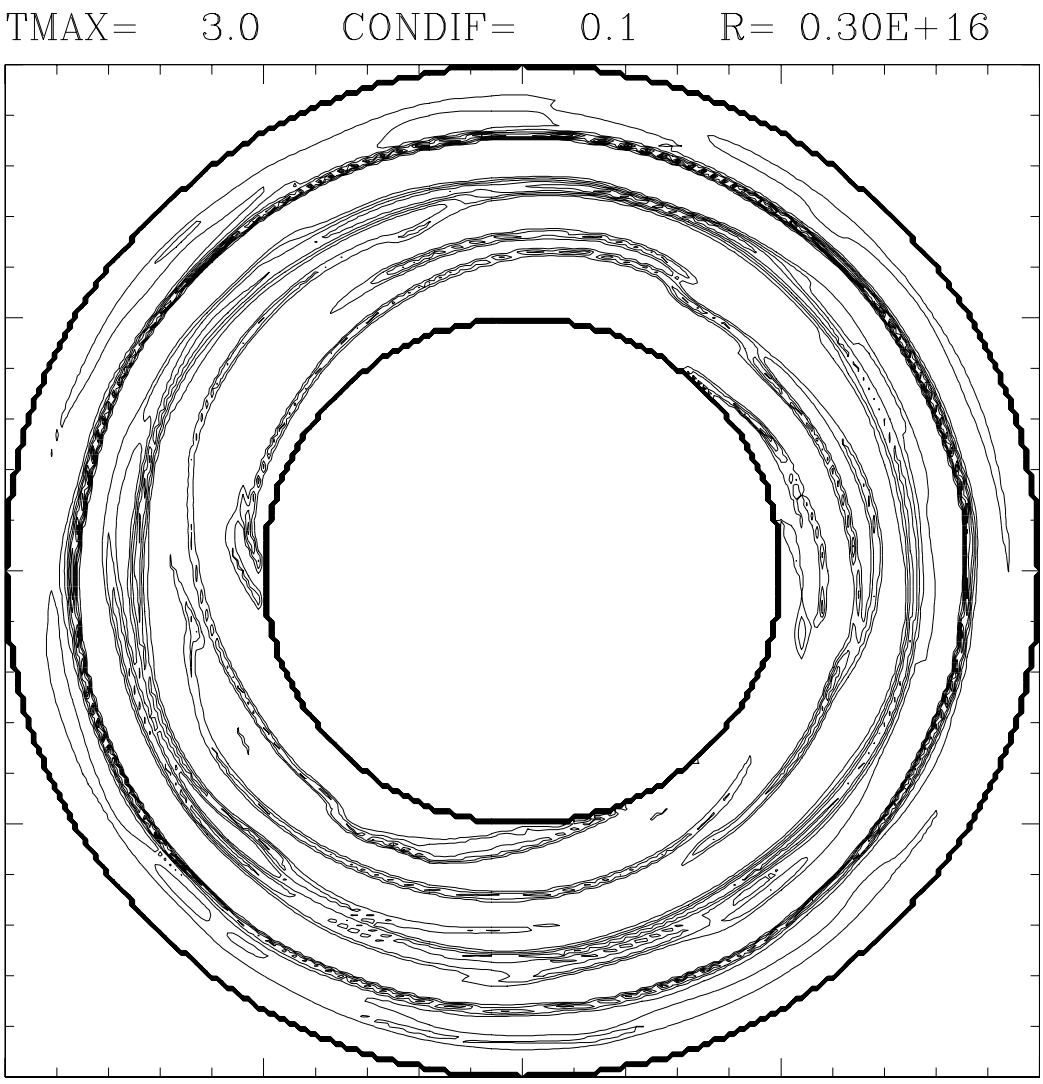

Fig. 3.— Equatorial temperature contours for model AH after 4000 yrs of evolution, as in Figure 1. Temperature contours represent factors of 1.3 change in temperature.

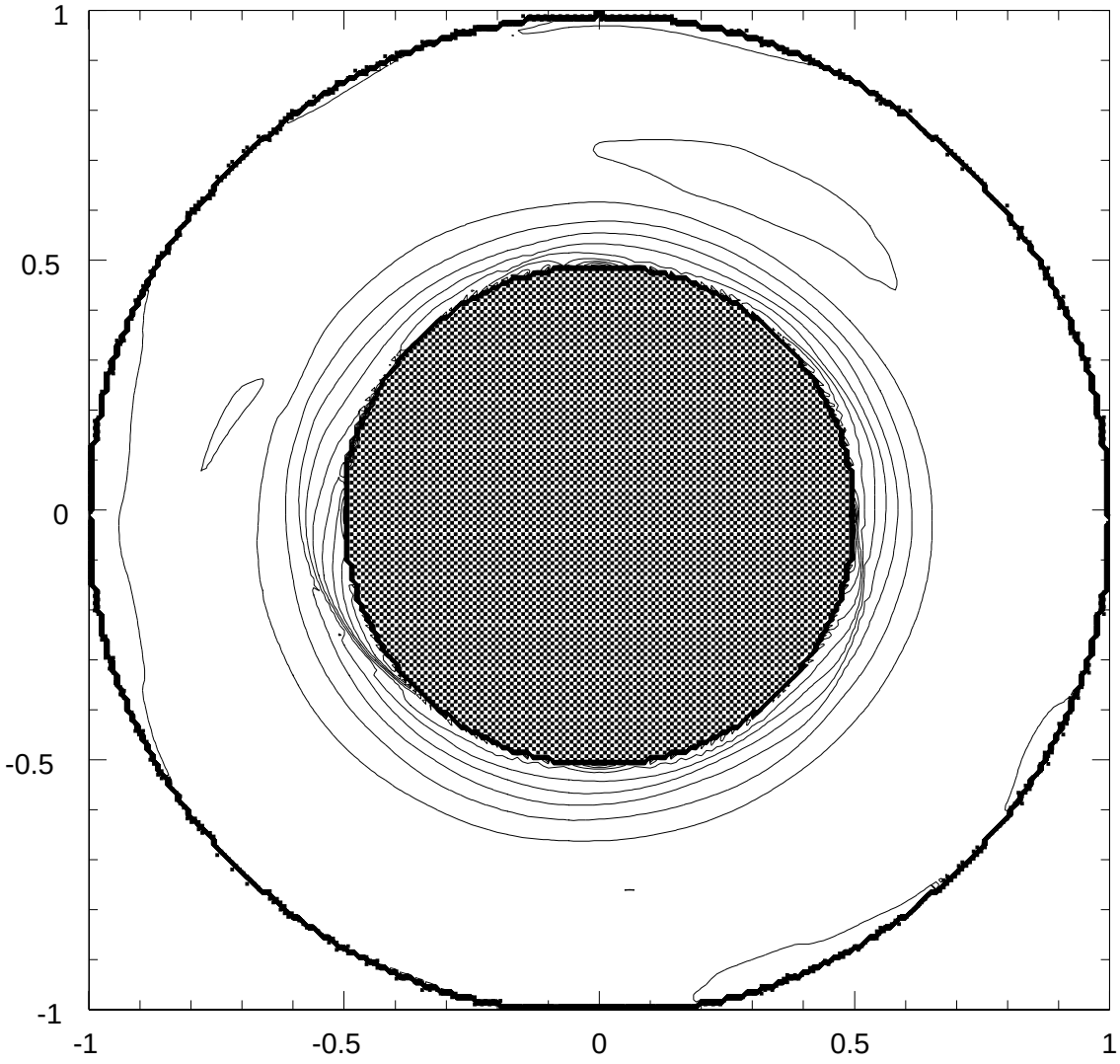

Fig. 4.— Equatorial density contours for model CH after 20000 yrs of evolution, as in Figure 1.

Table 1. Initial conditions for the models.

model	T_o (K)	$min(Q_i)$	N_ϕ	N_{Ylm}	t_f (yrs)
A	20	1.30	256	32	7,800
AH	20	1.30	512	48	4,000
B	25	1.45	256	32	35,000
BH	25	1.45	512	48	5,000
C	30	1.59	256	32	84,000
CH	30	1.59	512	48	20,000